IEEE Access
Multidisciplinary | Rapid Review | Open Access Journal

Received March 18, 2017, accepted April 9, 2017, date of publication April 24, 2017, date of current version June 7, 2017.

Digital Object Identifier 10.1109/ACCESS.2017.2696120

Triple-Mode Cavity Bandpass Filter on Doublet With Controllable Transmission Zeros

ZAI-CHENG GUO[1], SAI-WAI WONG[1], (Senior Member, IEEE), JING-YU LIN[1], (Student Member, IEEE), LEI ZHU[2], (Fellow, IEEE), QING-XIN CHU[1], (Senior Member, IEEE), QINGFENG ZHANG[3], (Senior Member, IEEE), AND YANG YANG[4], (Member, IEEE)

[1]School of Electronic and Information Engineering, South China University of Technology, Guangzhou 510640, China
[2]Department of Electrical and Computer Engineering, Faculty of Science and Technology, University of Macau, Macau 999078, China
[3]Department of Electronics and Electrical Engineering, South University of Science and Technology of China, Shenzhen 518055, China
[4]School of Computing and Communications, University of Technology Sydney, Ultimo, NSW 2007, Australia

Corresponding author: Sai-Wai Wong (wongsaiwai@ieee.org)

This work was supported in part by the National Natural Science Foundation of China under Grant 61327005, in part by the Department of Education of Guangdong Province Innovative Project under Grant 2015KTSCX010, and in part by the Guangzhou Science and Technology Project under Grant 201604016127.

ABSTRACT On the basis of doublet and its properties, a class of multiple-mode narrow band bandpasss filter is designed and fabricated by simultaneously exploiting the three resonant modes in a single rectangular cavity: TE_{101}, TE_{011}, and TM_{110} modes. The input/output ports of the proposed filter are fed by coupling a microstrip line to a slot on the side wall of a rectangular cavity. Different modes are excited by changing the position and shape of the two slots at input and output of the rectangular cavity without any intra-cavity coupling. Besides three poles within the passband, a pair of transmission zeros (TZs) is achieved, which can be controlled independently by setting the positions of the two TZs at the lower and/or upper stopband. High stopband attenuation and high filtering selectivity are achieved by considerably allocating three transmission poles and two zeros. In order to verify the proposed theory, two filter prototypes are fabricated and measured.

INDEX TERMS Doublet, triple-mode, rectangular cavity, bandpass filter, slots.

I. INTRODUCTION

Since the 1970s, multimode cavities have been widely used for designing various high-performance bandpass filters in many applications, such as satellite transponders, digital television broadcasting, and base stations [1]–[5]. As one of the advantages, a multimode cavity can be easily used for size and mass reduction. Hence, a large number of literature have been focusing on various bandpass filters with multimode cavities in the past few years [6]–[10].

On the other hand, high selectivity is specifically desired to create a very sharp roll-off response near the cut-off frequencies so as to reject unwanted out-of-band noise signals. Doublet [11], a specific coupling topology shown in Fig. 1, exhibits attractive zero-shifting features in terms of enhancing filter selectivity [12]. Based on doublet topology, some extended and modified doublets have been realized not only in cavities, but also in substrate integrated waveguide (SIW) and microstrip lines [13]–[16]. Higher-order filters, including bandpass or bandstop filters with symmetric and asymmetric pseudo-elliptic responses, can be designed by properly cascading doublets with resonators [11] or non-resonators [10], [17]. As such, one can design the separate sections as a module independently, thus providing much flexibility and convenience in filter design.

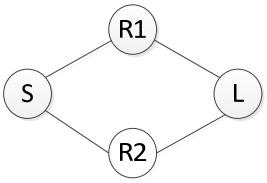

FIGURE 1. The basic coupling topology of a doublet.

In this paper, a doublet topology is realized in a multimode rectangular cavity operating in the TE_{101}, TE_{011} and TM_{110} modes, whose polarization directions of the electric-field are orthogonal to each other. Effectively allocating a slot at the input/output sections of a rectangular cavity,

the three different modes can be excited successfully. The design procedure of the proposed triple-mode cavity bandpass filter can be summarized as: a) proposing and analyzing, two doublets composed of different modes, b) generation of three transmission poles and two zeros by connecting two doublets in parallel. The excitation of triple modes in a single rectangular and the realization of negative coupling in a doublet are analyzed in detail. The proposed filter is realized in a very simple geometrical structure with good measurement results for both in-band and out-of-band performance.

II. PROPERTIES OF DOUBLET TOPOLOGY

Fig. 1 depicts the basic doublet, inclusive of two resonators, which are both coupled to the source and load in parallel without interaction with each other. Because of the two separate transmission paths between the source and load, the doublet topology can generate one TZ on either side of the desired passband. According to the coupling topology, a general coupling matrix of a doublet can be written as follows:

$$M = \begin{bmatrix} 0 & M_{S1} & M_{S2} & 0 \\ M_{S1} & M_{11} & 0 & M_{L1} \\ M_{S2} & 0 & M_{22} & M_{L2} \\ 0 & M_{L1} & M_{L2} & 0 \end{bmatrix} \tag{1}$$

The scattering parameters of this doublet can then be calculated using the following two equations [16]:

$$S_{21} = \frac{a\Omega + b}{\det} \tag{2}$$

$$S_{11} = \frac{\Omega^2 + c\Omega + d}{\det} \tag{3}$$

In (2) and (3), the symbol, Ω, denotes the normalized frequency of the low-pass prototype, and *det* is the determinant of the coupling matrix. The other four parameters, a, b, c and d, are constants related to the coupling coefficients in (1), which are given in [16]. For a given specification, the coupling matrix can be first synthesized based on the method in [18] and then the filtering responses can be calculated from (2) and (3).

In this topology, there are two points needed to be proclaimed. The first is the property that the position of its TZ can be shifted from one side of the passband to the other by detuning the resonators, meaning that the signs of M_{11} and M_{22} can be changed. This property is known as zero-shifting property as proven in [16] through the above two equations (2) and (3). The second point is that in order to realize one TZ out of the passband in a doublet, one negative coupling coefficient must be achieved [11] with condition below:

$$M_{S1}M_{S2}M_{L1}M_{L2} < 0 \tag{4}$$

In this context, three couplings must have the same sign and the remaining coupling is with opposite sign.

III. REALIZATION OF FILTER

In this part, a class of cavity filter prototypes is introduced. The excitation of first three resonant modes is studied to expound the design of the rectangular cavity filter. The cavity used herein is made up of silver plated aluminum, and filled with air. Each side of rectangular cavity is about one half wavelength in its respective resonant mode. The microstrip line is formed on a PCB with dielectric constant of 2.55, thickness of 0.8 mm and loss tangent of 0.003.

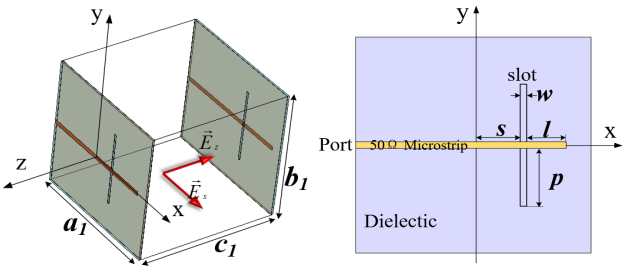

FIGURE 2. Three-dimensional view and side view of Type-A filter.

A. TYPE-A FILTER

A prototype is proposed as shown in Fig. 2, namely Type-A filter. The left figure is a three dimension (3-D) structural view and the right is its side view. In the 3-D view, the central part is a standard rectangular cavity, whose width, height, and length are marked as a_1, b_1, and c_1, respectively. A pair of symmetric 50 Ω open-ended microstrip lines are placed at the left-hand and right-hand sides of the cavity, respectively. A pair of rectangular slots, orthogonal to two microstrip feeding lines, are formed and opened on the side wall of the cavity. The slots at left and right sides of the cavity are both shifted along the positive X-axis, where the offset is marked as s. The distance between the end of the feed line and the slot is marked as l. From the side view, the two slots are overlapped and their dimensions are marked as w and p.

The configuration of Type-A filter, known as TE_{011}/TM_{110} dual-mode rectangular filter [16], is a doublet as there is no intra-cavity coupling and the electric-field polarizations of the two modes in cavity are orthogonal to each other. There exist two in-band poles and one out-of-band TZ. The property of zero-shifting could be realized by interchanging the width (a_1) and length (c_1) of the rectangular cavity, as shown in Fig. 3. Even though, there are still two crucial questions to be clarified: a) why the mode of TE_{011} and TM_{110} are excited, and b) how the negative coupling is realized in this filter.

For the first question, the excitation of the TE_{011} mode is attributed to the fact that the electromagnetic (EM) wave couples from the microstrip line to the slot with electric field component along X-axis $\overrightarrow{E_x}$, and it is the same as the electric field polarization direction of TE_{011} mode, so TE_{011} mode is excited. As for the excitation of TM_{110} mode, Fig. 4 is presented showing the electric field above the slot line. It could be considered that the slot divided the bottom of the PCB into two parts: part 1 and part 2, as shown in the bottom of Fig. 4. When the slot is located at the center, part 1 and part 2 are symmetric to the slot. The magnitudes

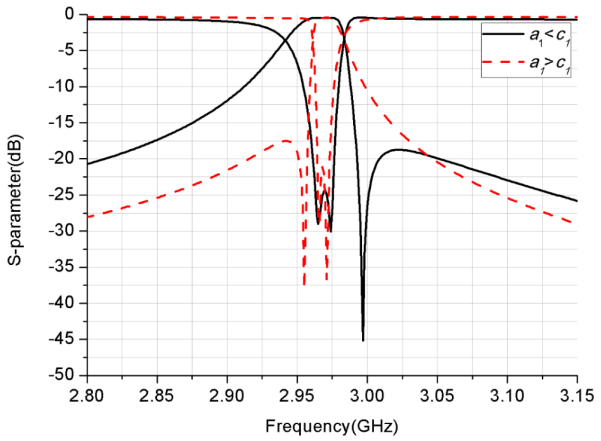

FIGURE 3. Type-A filter: zero-shifting by interchanging width (a_1) and length (c_1).

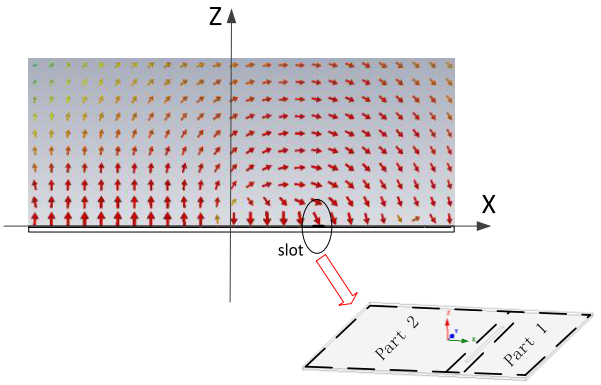

FIGURE 4. Type-A filter: slot used for dividing the bottom of the PCB into two distinctive parts.

of their electric strength of each part are equal to each other when the slot mode is excited. The electric field components at Z-axis direction of the part 1 and part 2 have the same magnitude but opposite sign, leading to complete electric field cancellation along the Z-axis. Thus, there is no net electric field component in the Z-axis. When the slot is shifted slightly along the X-axis, the two parts are asymmetric and their magnitudes are different between part 1 and part 2 as shown in Fig. 4. Though the directions of the electric field at part 1 and part 2 are still opposite, there is a non-zero electric field in the Z-axis after electric field cancellation of part 1 and part 2, which can be found from the electric field between part 1 and part 2 in Fig. 4. Actually, the offset could be regarded as a perturbation for electric field along the Z-axis to excite the resonant mode with electric component along the Z-axis. The mode TM_{110} has this electric field direction and meet the resonance condition, thus it can be excited.

For the second question, it can be expounded by Fig. 5. In Fig. 5(a), the positions of the slots and the magnetic field of the two modes, namely TE_{011} and TM_{110}, are demonstrated. The magnetic field directions of TE_{011} (resonator $R1$) at the two slots are opposite, which means the signs of M_{S1} and M_{L1}

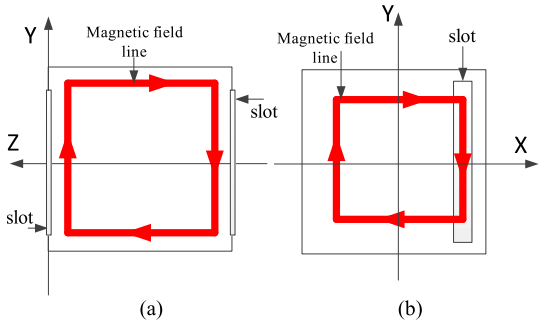

FIGURE 5. The magnetic field of Type-A filter (a) TE_{011} mode, (b) TM_{110} mode.

in coupling matrix (1) are opposite. While in Fig. 5(b), the two slots are overlapped and the magnetic field directions of TM_{110} (resonator $R2$) at the two slots are same, so the signs of M_{S2} and M_{L2} are same as each other [11], [19]. As such, the four couplings all satisfy the condition in (4) to generate one TZ out of the desired passband.

TABLE 1. Position of TZ for Type-A filter.

Length of size	a_1 c_1	a_1 c_1
Position of TZ	left	right

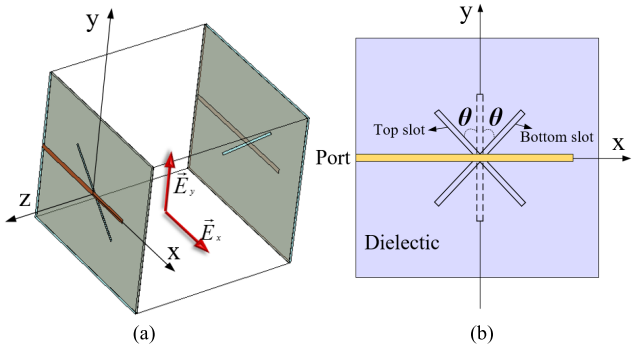

FIGURE 6. (a) 3-D view of Type-B filter, and (b) rotated slots with angle θ on Type-A filter.

As a summary, the relation of TZ is concluded in TABLE 1. When width (a_1) of the cavity is larger than length (c_1), TZ is at the lower stopband. Conversely, when the width is less than the length, TZ is at the higher stopband.

B. TYPE-B FILTER

The structure of Type-B filter is shown in Fig. 6. The center of two slots are set as the origin and the slot at the left-hand side is rotated counterclockwise with an angle θ around the Z-axis, while the slot at the right-hand side is rotated clockwise with θ around the Z-axis. The two slots are symmetric with respect to the Y-axis in the XY- plane. Fig. 6(a) displays the 3-D view of Type-B filter.

In this Type-B filter, the dual modes excited here are TE_{101} and TE_{011} as described in [20]. There exist

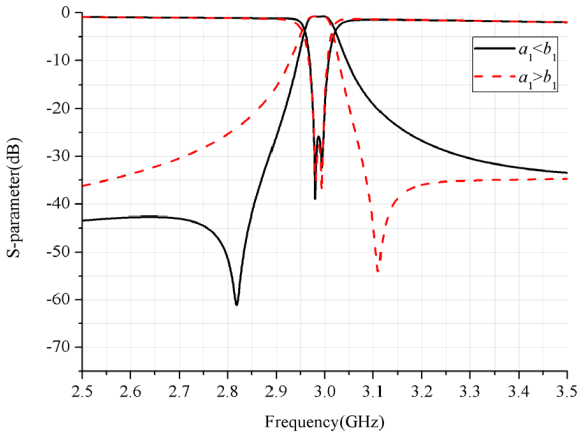

FIGURE 7. Type-B filter: zero-shifting by interchanging width (a_1) and height (b_1).

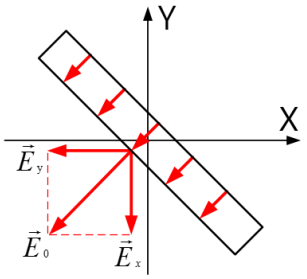

FIGURE 8. Electric field vector $\vec{E_0}$ in the slot with two orthogonal components along X-axis $\vec{E_x}$ and Y-axis $\vec{E_y}$.

two in-band poles and one out-of-band TZ. Fig. 7 shows that the property of zero-shifting could be realized by interchanging the width (a_1) and height (b_1) of the rectangular cavity. Fig. 8 is prepared to explain how the two modes are excited. The electric field vector in the slot at the left side of the cavity is perpendicular to the long side of the slot under the assumption that the vector $\vec{E_0}$, can be resolved into two components along the X-axis (marked as $\vec{E_x}$) and Y-axis (marked as $\vec{E_y}$). The electric field direction of $\vec{E_x}$ is the same as that of TE_{011} mode, so the component vector $\vec{E_x}$ can excite TE_{011} mode. Similarly, the electric field direction of $\vec{E_y}$ is the same as that of TE_{101} mode, so $\vec{E_y}$ can excite TE_{101} mode. Similar to Type-A filter, Type-B filter is also a doublet, and it has the TZ zero-shifting property by interchanging the width (a_1) and height (b_1).

In order to explain the negative coupling of this doublet, Fig. 9 is provided. In the case of Type-B filter, the negative coupling results from the phase reversal of one component vector in the slots. From Fig. 8, we can understand that the electric field vector in each slot could be resolved into two components ($\vec{E_x}$ and $\vec{E_y}$), which correspond to the two resonators of the doublet. There are two cases in total in terms of the electric field in the two slots as shown in Fig.9. It could be seen that no matter which case is, there is only one phase

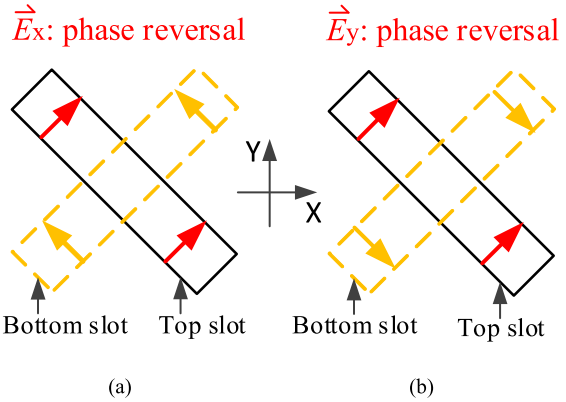

FIGURE 9. The electric field of Type-B filter in slots of two cases: (a) $\vec{E_x}$: phase reversal, (b) $\vec{E_y}$: phase reversal.

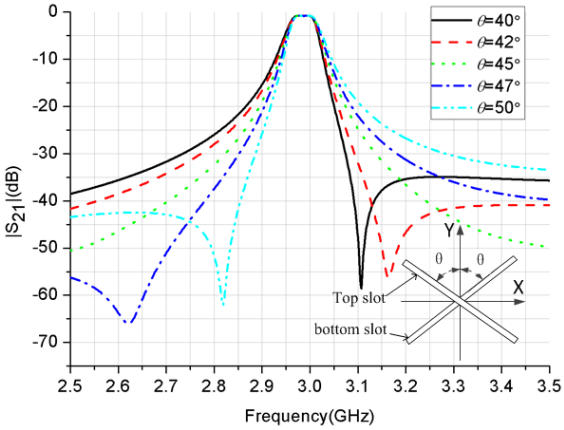

FIGURE 10. Simulated response $|S_{21}|$ of filter Type-B under different θ.

reversal of one component vector. It means that one resonator of the doublet produces opposite sign of coupling between the source and load, while the other resonator keeps the same. Thus, the assumption $M_{S1}M_{L1}M_{S2}M_{L2} < 0$ is hold, leading to the emergence of one TZ in the stopband.

The effect of the rotated angle θ is provided in Fig.10. By changing θ, one TZ could be produced on either side of the core passband. When θ is smaller than 45° or increases from 40° to 42°, the TZ at upper-stopband moves upwards. Similarly when θ is larger than 45° or increases from 47° to 50°, the TZ at lower- stopband moves to the higher band. When θ equals to 45°, there is no TZ. In other word, when θ is larger or less than 45°, one TZ will appear at either lower or higher stopband. As θ gets far away from 45°, the TZ gets close to the passband. This phenomenon could be explained through (2). In this case, we could set $M_{S1} = M_{L1}$ and $M_{S2} = -M_{L2}$ as the consequence of symmetry of the two resonators, then we could get the following expression:

$$S_{21} = \frac{(M_{S2}^2 - M_{S1}^2)\Omega + (M22M_{S2}^2 - M_{11}M_{S1}^2)}{\det} \quad (5)$$

It could be seen herein that when $M_{S1} = M_{S2}$, the numerator of (5) is a constant, so the value of S_{21} is not possible zero, which implies no TZ, corresponding to the situation

of $\theta = 45°$. For a cubic cavity, the couplings are mutually related to each other as investigated in [20].

$$\tan(\theta) = \frac{M_{S2}}{M_{S1}} \tag{6}$$

For simplicity, $M_{11} = -M_{22}$ is assumed to indicate that the resonant frequency of resonator $R1$ has the same offset from the center frequency as that of resonator $R2$. Then, under the condition of $S_{21} = 0$, we could obtain the frequency of TZ:

$$\Omega_z = M_{11}\frac{\tan^2(\theta) - 1}{\tan^2(\theta) + 1} \tag{7}$$

where Ω_Z stands for the normalized frequency of TZ.

From (7), it could be seen that the position of TZ could appear on either the upper or lower side of the passband by properly selecting the rotated angle θ. It needs to be noteworthy that the threshold value of the rotated angle θ is not remained at 45° when TZ vanishes, but it mainly depends on the size of rectangular cavity. According to (7), the threshold value of θ could be deduced as the angle that makes M_{S1} equal to M_{S2}. When the width (a_1) is approximately equal to the height (b_1), the threshold of θ is equal to about 45°. However, if the width is much less or larger than height, the threshold value is pushed far away from 45°. The following study will be executed under the assumption that the width (a_1) is approximately equal to height (b_1), so the threshold of θ is remained as about 45°.

TABLE 2. Position of TZ for Type-B filter.

Position of TZ	a_1 b_1	a_1 b_1
θ 45	right	left
θ 45	left	right

In summary, the above investigation and analysis can be drawn in TABLE 2 for the relationship between the positions of TZs with θ, a_1 and b_1.

C. TYPE-C FILTER

Now, we know that the rotated angle in the XY- plane of the slots would excite the resonant modes with electric field in the X- and Y-axes. Offsetting the slot position from the origin, the mode in the Z-axis could be excited. This inspires us to combine these two excitation methods to form a triple-mode bandpass filter, namely Type-C. Its 3-D view is provided in Fig. 11. The slots in Type-C filter have the same-direction offset of Type-A filter and an oppositely rotated angle of Type-B filter. The offset and rotated angle are marked as s and θ, respectively.

By combining the Type-A and Type-B filters, Type-C filter could be comprised by shunt connecting two doublets in parallel, as shown in Fig. 12. In this way, it is found that Type-C filter could maintain the characteristics of the two previous filters, which means that there exist three modes within passband and two TZs outside the passband. Furthermore, the two TZs could be controlled independently by the two doublets, respectively. According to TABLE 1 and 2,

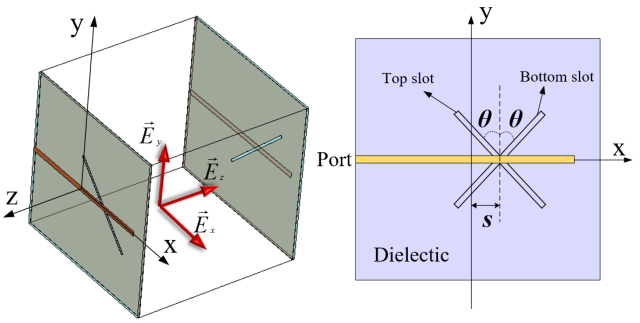

FIGURE 11. Crossed slots and three-dimensional view of Type-D filter.

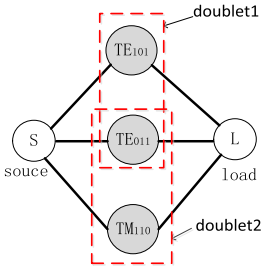

FIGURE 12. Coupling topology of the proposed triple-mode filter.

TABLE 3. Position of TZs for Type-C filter.

Position of TZs	c_1 a_1 b_1	c_1 a_1 b_1
θ 45	One TZ at left, one TZ at right	One TZ at left, one TZ at right
θ 45	Two TZs at right	Two TZs at left

we obtain an integrated result about the position of TZs for Type-C filter as tabulated in TABLE 3. There are four cases about the positions of the two TZs in Type-C filter. For the first case: $c_1 > a_1 > b_1$ and $\theta < 45°$, the TZ in doublet 1 tends to appear on the left of the passband, and the TZ in doublet 2 appears on the right of the passband. For the second case: $c_1 < a_1 < b_1$ and $\theta < 45°$, the two TZs in the first case are interchanged with each other, but the final filtering response keeps unchanged. For the third case: $c_1 > a_1 > b_1$ and $\theta > 45°$, the two TZs both appear on the right of the passband, corresponding to the upper-stopband. For the fourth case: $c_1 < a_1 < b_1$ and $\theta > 45°$, the two TZs both moves to the left of passband, corresponding to the lower stopband.

In this context, it needs to be explained why there are four cases in TABLE 3. In order to produce the two TZs from the Type-A and Type-B filters corresponding to TE_{011} and TM_{110} modes of Type-A, and TE_{011} and TE_{101} modes of Type-B, the TE_{011} mode should be located in the middle of the three modes because TE_{011} mode is shared by both the doublets as shown in Fig. 12. Thus, there are only two cases for the lengths of the three sides of the cavity: $b_1 < a_1 < c_1$ or $c_1 < a_1 < b_1$, according to equations (8)-(10) :

$$(K_{1,0,1})^2 = \left(\frac{\pi}{a1}\right)^2 + \left(\frac{\pi}{c1}\right)^2 \tag{8}$$

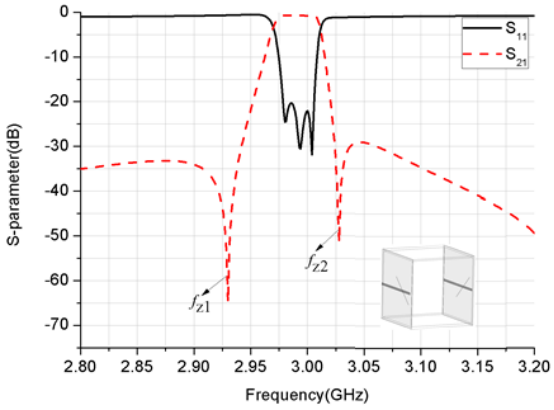

FIGURE 13. Simulated result of Type-C filter with the first case: $b_1 < a_1 < c_1$ and $\theta < 45°$.

$$(K_{1,1,0})^2 = (\frac{\pi}{a1})^2 + (\frac{\pi}{b1})^2 \tag{9}$$

$$(K_{0,1,1})^2 = (\frac{\pi}{b1})^2 + (\frac{\pi}{c1})^2 \tag{10}$$

where $K_{m,n,p}$ represents the wavenumber of these three resonant modes with m, n and p equal to 0 or 1.

It needs to be noted that if a TZ appears within the passband, no single passband with three poles can be formed. In addition, the value of θ around 45° probably affects the position of one TZ, so there are four cases in total as listed in TABLE 3. In the following, we will study these four cases, respectively.

Fig. 13 represents the simulated result for the first case: $b_1 < a_1 < c_1$ ($a_1 = 70.9$ mm, $b_1 = 70$ mm, $c_1 = 72$ mm) and the rotated angle: $\theta < 45°$ (e.g. $\theta = 40°$). In the previous study, it's understood that TZ f_{z1} is contributed by the doublet 1, while TZ f_{z2} is contributed by the doublet 2. Moreover, the positions of the two TZs are mainly controlled by the rotated angle θ and offset s, respectively. As a result, by regulating the rotated angle θ and offset s, the positions of the two TZs can be well controlled. This can also demonstrate the validity of TABLE 3.

For the second case, we appropriately choose the length of three sides: $c_1 < a_1 < b_1$ (e.g. $a_1 = 71$ mm, $b_1 = 72$ mm and $c_1 = 70$ mm) and the rotated angle: $\theta < 45°$ (e.g. $\theta = 40°$) according to the data listed in TABLE 3. The derived results show the similar responses as those in the first case. Herein, the first TZ (f_{z1}) is contributed by doublet 1, and the second TZ (f_{z2}) is contributed by doublet 2, which is the reverse sequence in the first case.

For the third case, we choose the length of three sides as: $b_1 < a_1 < c_1$ ($a_1 = 71.4$ mm, $b_1 = 70$ mm, $c_1 = 71.8$ mm) and the rotated angle: $\theta > 45°$ ($\theta = 49°$), according to TABLE 3. The simulated results are plotted in Fig. 14. There are three poles within passband and two TZs at the higher stopband.

For the fourth case, we choose the case of $c_1 < a_1 < b_1$ ($a_1 = 71$ mm, $b_1 = 72.2$ mm, $c_1 = 70.5$ mm) and the rotated angle: $\theta > 45°$ ($\theta = 50°$), from TABLE 3. The simulated

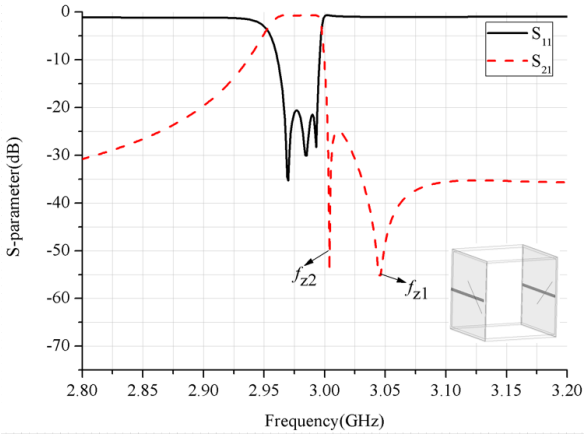

FIGURE 14. Simulated result of filter Type-C with the third case: $b < a < c$ and $\theta > 45°$.

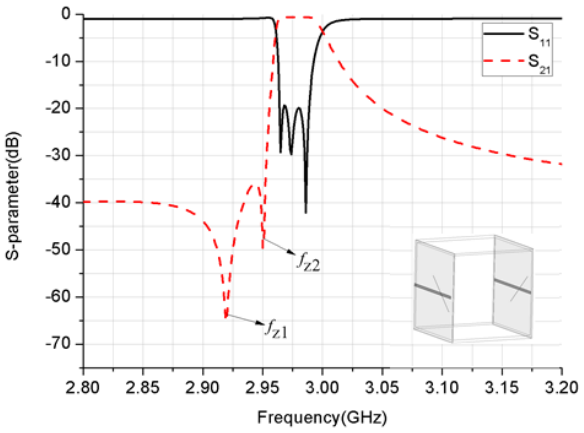

FIGURE 15. The simulation result of filter Type-C with the fourth case: $c_1 < a_1 < b_1$ and $\theta > 45°$.

results are illustrated in Fig. 15 with three modes within passband and two TZs in the lower stopband.

In summary, the positions of the two TZs can be effectively determined by changing the relative length of three sides of the rectangular cavity and the position of the slots. Two crucial parameters, i.e., rotated angle θ and offset s, are used to control the frequencies of the two TZs, respectively. Our simulated results show that the return loss of all the studied filters is better than 20 dB and the respective insertion loss is less than 1 dB. Due to the two elaborately generated TZs, the presented filters have attractive highly-attenuated out-of-band performance near the lower and upper cut-off frequencies.

IV. RESULTS AND VALIDATION

In order to demonstrate the validity of the design, two kinds of filters are fabricated and measured in this part. In these designs simulated results are implemented by CST microwave studio.

For a specification of the center frequency at 3 GHz, bandwidth of 95 MHz, 15-dB return loss, and two TZs at 2.87/3.08 GHz, the matrix of normalized angular frequency

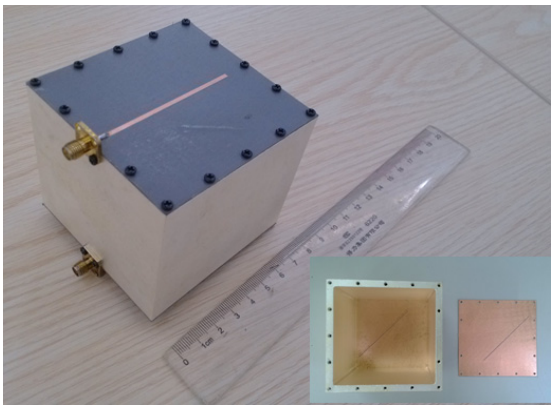

FIGURE 16. Pictures of the fabricated filter of Type-C in a single block.

of low-pass prototype filter can be formed and synthesized as [18]:

$$\mathrm{M} = \begin{bmatrix} 0 & -0.4538 & 0.7161 & -0.3875 & 0 \\ -0.4538 & 1.2395 & 0 & 0 & 0.4538 \\ 0.7161 & 0 & -0.1191 & 0 & 0.7161 \\ -0.3875 & 0 & 0 & -1.2123 & 0.3875 \\ 0 & 0.4538 & 0.7161 & 0.3875 & 0 \end{bmatrix} \tag{11}$$

According to (11), a filter of the first case is designed and fabricated. In Fig. 16, a subset picture shows the internal view of the fabricated cavity. The comparison among the simulated, measured and coupling-matrix results is provided in Fig. 17. For the measured results, the achieved passband has the center frequency of 3 GHz, 60 MHz absolute bandwidth, 2.2 dB insertion loss and more than 20 dB return loss. Moreover, two TZs appear at about 2.88 and 3.08 GHz, respectively. With the help of the two TZs, attenuation at both sides of the passband achieves more than 25 dB. The slight offset of the TZ position located at upper stopband between measured results and simulated results or matrix is caused by measurement error. Meanwhile due to the microstrip line feeding, the return loss and insertion loss of the measured result are higher than the simulation result.

From the requirement of different cases of Type-C filter as shown in TABLE 3, it is found that the first and the third cases of a single block have the same requirement as a rectangular metal cavity ($b_1 < a_1 < c_1$). But, there is a different requirement in the rotated angle θ of the two cases: i.e., $\theta < 45°$ for the first case and $\theta > 45°$ for the third case. By changing different input/output microstrip lines, we can realize two filters with different positions of TZs using one single cavity. In this way, a filter in the third case is fabricated and measured by sharing the same rectangular metal cavity. Fig. 18 depicts the comparison between the simulated and measured results for the third case. The measured center frequency is at 3 GHz with a bandwidth of 50 MHz. The insertion loss is about 2.3 dB and return loss is higher than 20.0 dB in the desired passband. Compared to Fig. 17 of the first case, the two TZs are both at the upper stopband, and they are equal to about

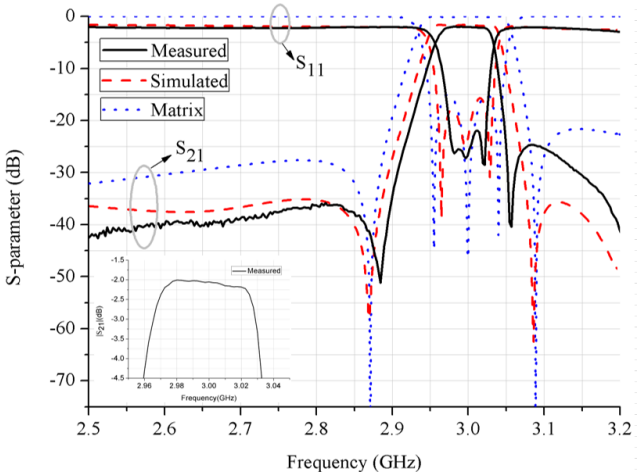

FIGURE 17. Comparison between the measured and the simulated results for the first case.

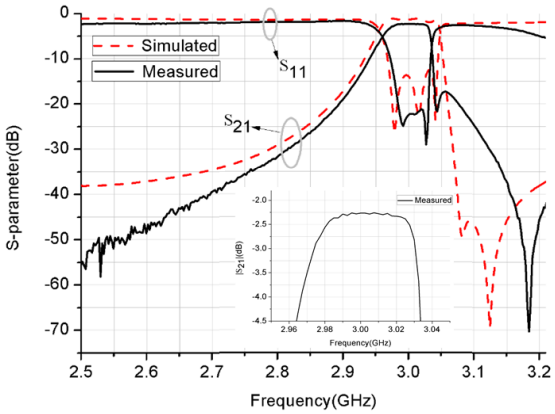

FIGURE 18. Comparison between the measured and the simulated results for the third case.

3.04 and 3.18 GHz, respectively. The out-of-band attenuation exceeds 17 dB. The same to fig. 17, the slight offset of the TZ position located at upper stopband between measured results and simulated results or matrix is caused by measurement error. Meanwhile due to the microstrip feed, the return loss and insertion loss of the former are higher than that of the latter.

TABLE 4. Parameters for the two cases.

	l	P	W	s	θ
Case I	21 mm	26 mm	0.3 mm	13 mm	38
Case III	18 mm	33 mm	0.3 mm	9 mm	46

The dimensions of the rectangular cavity are as followed: $a_1 = 70.8$ mm, $b_1 = 68.5$ mm and $c_1 = 72.8$ mm, and the specific parameters of the microstrip line for the two cases are listed in TABLE 4. Once the parameters are determined, the unloaded quality factor of each mode could be calculated and they are equal to 3684 for TE_{101}, 2281 for TE_{011}, and 4392 for TM_{110}, respectively. For both cases, there are some visible

deviations between the simulated and measured results in term of bandwidth and the frequencies of the TZs in Fig. 17 and Fig. 18. This is mainly due to unavoidable tolerance during fabrication and experimental set-up.

V. CONCLUSION

In this paper, by utilizing three fundamental resonant modes (TE_{011}, TE_{101} and TM_{110}) in a single rectangular metal cavity, two kinds of doublets are presented and designed by connecting the two doublets in parallel. The triple-mode filter with two TZs is proposed and implemented. Extensive studies have been focused on the investigation of doublet realization, such as the excitation of different modes and realization of negative couplings, such as proper reallocation of different TZs in either lower or upper stopband. By installing the slots at the bottom of the PCB and changing their location, different resonant modes could be excited simultaneously with negative couplings for doublets realization. Two crucial parameters, namely, rotated angle θ and offset s of the slots, as well as the zero-shifting property of a doublet are utilized to create a few TZs at the desired bands. By controlling these parameters, the two TZs could be arbitrarily placed in the lower and/or upper stopband as desired. Four kinds of filters are designed to achieve three in-band poles and two out-of-band TZs. Because of the elaborately designed TZs, the designed filters have a sharp roll-off frequency response in the transitional band. Two prototypes are fabricated and measured. Both the measured results are found in good agreement with the simulated ones, demonstrating the validity of our design methods.

REFERENCES

[1] A. E. Williams, "A four-cavity elliptic waveguide filter," *IEEE Trans. Microw. Theory Techn.*, vol. 18, no. 12, pp. 1109–1114, Dec. 1970.
[2] A. E. Atia and A. E. Williams, "New types of waveguide bandpass filters for satellite transponders," *Comsat Tech. Rev.*, vol. 1, no. 1, pp. 20–43, 1971.
[3] A. E. Atia and A. E. Williams, "Narrow-bandpass waveguide filters," *IEEE Trans. Microw. Theory Techn.*, vol. 20, no. 4, pp. 258–265, Apr. 1972.
[4] K. Konno, M. Kubota, and Y. Iwamoto, "A compact elliptic-function BPF using triple-mode cavities for terrestrial digital television transmitters," in *IEEE MTT-S Int. Microw. Symp. Dig.*, May 2001, pp. 1321–1324.
[5] C. Wang, W. Wilber, and B. Engst, "A practical triple-mode monoblock bandpass filter for base station applications," in *IEEE MTT-S Int. Microw. Symp. Dig.*, May 2001, pp. 1783–1786.
[6] X.-X. Liang, K. A. Zaki, and A. E. Atia, "Dual mode coupling by square corner cut in resonators and filters," *IEEE Trans. Microw. Theory Techn.*, vol. 40, no. 12, pp. 2294–2302, Dec. 1992.
[7] G. Lastoria, G. Gerini, M. Guglielmi, and F. Emma, "CAD of triple-mode cavities in rectangular waveguide," *IEEE Microw. Guided Wave Lett.*, vol. 8, no. 10, pp. 339–341, Oct. 1998.
[8] G. Gerini, F. D. Bustamante, and M. Guglielmi, "Triple mode filters with coaxial excitation," in *IEEE MTT-S Int. Microw. Symp. Dig.*, Jun. 2000, pp. 1763–1766.
[9] M. H. Chen, "Short-circuit tuning method for singly terminated filters," *IEEE Trans. Microw. Theory Techn.*, vol. 25, no. 12, pp. 1032–1036, Dec. 1977.
[10] S. Amari and U. Rosenberg, "New in-line dual- and triple-mode cavity filters with nonresonating nodes," *IEEE Trans. Microw. Theory Techn.*, vol. 53, no. 4, pp. 1272–1279, Apr. 2005.
[11] S. Amari and U. Rosenberg, "The doublet: A new building block for modular design of elliptic filters," in *Proc. 32nd Eur. Microw. Conf.*, vol. 2. Milan, Italy, Sep. 2002, pp. 1–3.
[12] S. Amari, G. Tadeson, J. Cihlar, R. Wu, and U. Rosenberg, "Pseudo-elliptic microstrip line filters with zero-shifting properties," *IEEE Microw. Wireless Compon. Lett.*, vol. 14, no. 7, pp. 346–348, Jul. 2004.
[13] W. Shen, X.-W. Sun, W.-Y. Yin, J.-F. Mao, and Q.-F. Wei, "A novel single-cavity dual mode substrate integrated waveguide filter with non-resonating node," *IEEE Microw. Wireless Compon. Lett.*, vol. 19, no. 6, pp. 368–370, Jun. 2009.
[14] S. Amari and U. Rosenberg, "A universal building block for advanced modular design of microwave filters," *IEEE Microw. Wireless Compon. Lett.*, vol. 13, no. 12, pp. 541–543, Dec. 2003.
[15] K. Shen, G.-M. Wang, S.-H. Fu, and G.-D. Gu, "Highly selective bandpass filter based on substrate integrated waveguide," *Electron. Lett.*, vol. 45, no. 14, pp. 746–748, Jul. 2009.
[16] U. Rosenberg and S. Amari, "Novel coupling schemes for microwave resonator filters," *IEEE Trans. Microw. Theory Techn.*, vol. 50, no. 12, pp. 2896–2902, Dec. 2002.
[17] S. Bastioli, "Nonresonating mode waveguide filters," *IEEE Microw. Mag.*, vol. 12, no. 6, pp. 77–86, Oct. 2011.
[18] R. J. Cameron, "Advanced coupling matrix synthesis techniques for microwave filters," *IEEE Trans. Microw. Theory Techn.*, vol. 51, no. 1, pp. 1–10, Jan. 2003.
[19] U. Rosenberg, "New 'Planar' waveguide cavity elliptic function filters," in *Proc. 25th Eur. Microw. Conf.*, Bologna, Italy, Sep. 1995, pp. 524–527.
[20] S. Amari and M. Bekheit, "New dual-mode dielectric resonator filters," *IEEE Microw. Wireless Compon. Lett.*, vol. 15, no. 3, pp. 162–164, Mar. 2005.

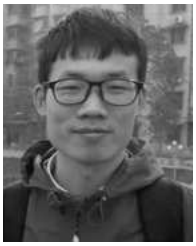

ZAI-CHENG GUO received the B.S. degree and the master's degree in electronic engineering from the South China University of Technology, Guangzhou, China, in 2013 and 2016, respectively.

He is currently pursuing the Ph.D. degree with Macau University, Macau. In 2016, he was with the Southern University of Science and Technology, Shenzhen, as an Exchange Student. In 2016, he was with Macau University as a Research Assistance. He was a recipient of the Graduate National Scholarship in 2015.

SAI-WAI WONG (S'06–M'09–SM'14) received the B.S. degree in electronic engineering from The Hong Kong University of Science and Technology, Hong Kong, in 2003, and the M.Sc. and Ph.D. degrees in communication engineering from Nanyang Technological University, Singapore, in 2006 and 2009, respectively.

From 2003 to 2005, he was the Lead of the Engineering Department in mainland of China with two manufacturing companies in Hong Kong. From 2009 to 2010, he was a Research Fellow with the Institute for Infocomm Research, Singapore. In 2016, he was a Visiting Professor with the City University of Hong Kong, Hong Kong. Since 2010, he has been an Associate Professor and became a Full Professor with the School of Electronic and Information Engineering, South China University of Technology, Guangzhou, China. His current research interests include RF/microwave circuit and wideband antenna design.

Dr. Wong was a recipient of the New Century Excellent Talents in University Award in 2013. He is a Reviewer for several top-tier journals.

JING-YU LIN (S'14) was born in Quanzhou, China, in 1993. He received the B.S. degree in information security from Southwest Jiaotong University, Chengdu, China, in 2016. He is currently pursuing the M.S. degree with the School of Electronic and Information Engineering, South China University of Technology, Guangzhou, China.

His current research interests include cavity microwave filters and multiplexers design.

LEI ZHU (S'91–M'93–SM'00–F'12) received the B.Eng. and M.Eng. degrees in radio engineering from Southeast University, Nanjing, China, in 1985 and 1988, respectively, and the Ph.D. degree in electronic engineering from the University of Electro-Communications, Tokyo, Japan, in 1993.

From 1993 to 1996, he was a Research Engineer with Matsushita-Kotobuki Electronics Industries Ltd., Tokyo. From 1996 to 2000, he was a Research Fellow with the Faculty of Engineering, École Polytechnique de Montréal, University of Montreal, QC, Canada. From 2000 to 2013, he was an Associate Professor with the School of Electrical and Electronic Engineering, Nanyang Technological University, Singapore. Since 2013, he has been a Professor with the Faculty of Science and Technology, University of Macau, Macau, China. Since 2014, he has been the Head of the Electrical and Computer Engineering Department, University of Macau.

He has authored or co-authored 246 papers in peer-reviewed journals and conference proceedings, including 80 papers in the IEEE transactions/letters/magazines. His published papers have been cited over 3,088 times with the H-index of 31 and average citations per paper of 18.18 (source: ISI Web of Science). His research interests include microwave circuits, antenna technique, and applied electromagnetics.

Dr. Zhu has been a member of the IEEE MTT-S Technical Committee on Computer-Aided Design since 2006 and a member of the IEEE MTT-S Fellow Evaluation Committee since 2013. He was a recipient of the 1997 Asia-Pacific Microwave Prize Award, the 1996 Silver Award of Excellent Invention from the Matsushita-Kotobuki Electronics Industries Ltd., and the 1993 First-Order Achievement Award in Science and Technology from the National Education Committee, China. He served as the General Chair of the 2008 IEEE MTT-S International Microwave Workshop Series on the Art of Miniaturizing RF and Microwave Passive Components, Chengdu, China, and a Technical Program Committee Co-Chair of the 2009 Asia-Pacific Microwave Conference, Singapore. He was an Associate Editor of the *IEICE on Electronics* from 2003 to 2005, an Associate Editor of the IEEE Microwave and Wireless Components Letters from 2006 to 2012, and an Associate Editor of the IEEE Transactions on Microwave Theory and Techniques from 2010 to 2013.

QING-XIN CHU (M'99–SM'11) received the B.S., M.E., and Ph.D. degrees in electronic engineering from Xidian University, Xi'an, China, in 1982, 1987, and 1994, respectively.

From 1982 to 2004, he was with the School of Electronic Engineering, Xidian University, where he has been a Professor and the Vice Dean since 1997. He has been a Distinguished Professor of the Shaanxi Hundred-Talent Program with Xidian University since 2011. He is currently a Chair Professor with the School of Electronic and Information Engineering, South China University of Technology, where he is also the Director of the Research Institute of Antennas and RF Techniques and the Chair of the Engineering Center of Antennas and RF Techniques, Guangdong.

He has authored over 300 papers in journals and conferences, which were indexed in SCI over 1,500 times. One of his papers published in the IEEE Transactions on Antennas and Propagations in 2008 became the top Essential Science Indicators paper within ten years in the field of antenna (SCI indexed self-excluded in the antenna field ranged top 1%). He holds over 30 invention patents of China. He is a Senior Member of the China Electronic Institute. In 2014, he was elected as the Highly Cited Scholar by Elsevier in the field of electrical and electronic engineering. He is the Foundation Chair of the IEEE Guangzhou AP/MTT Chapter.

Dr. Chu was a recipient of the Science Award by Guangdong in 2013, the Science Awards by the Education Ministry of China in 2008 and 2002, the Fellowship Award by Japan Society for Promotion of Science in 2004, the Singapore Tan Chin Tuan Exchange Fellowship Award in 2003, and the Educational Award by Shaanxi in 2003.

His current research interests include antennas in wireless communication, microwave filters, spatial power combining array, and numerical techniques in electromagnetics.

QINGFENG ZHANG (S'07–M'11–SM'15) was born in Changzhou, China. He received the B.E. degree in electrical engineering from the University of Science and Technology of China, Hefei, China, in 2007, and the Ph.D. degree in electrical engineering from Nanyang Technological University, Singapore, in 2011.

From 2011 to 2013, he was with the Poly-Grames Research Center, École Polytechnique de Montréal, Montréal, QC, Canada, as a Post-Doctoral Fellow. Since 2013, he has been with the South University of Science and Technology of China, Shenzhen, China, as an Assistant Professor. His research interests are focused on emerging novel electromagnetics technologies and multidisciplinary topics.

YANG YANG (S'11–M'14) received the Ph.D. degree from Monash University, Melbourne, Australia, in 2013. From 2012 to 2015, he was an Asia-Pacific GSP Engineer with Rain Bird. He was a Senior Research Associate with the Department of Engineering, Macquarie University, from 2015 to 2016. In 2016, he was a Research Fellow with the State Key Laboratory of Millimeter-Waves, City University of Hong Kong. Since 2016, he has been a Lecturer with the University of Technology Sydney. His research interests include microwave and millimeter-wave circuits, reconfigurable antennas, wearable antennas, biosensors, and sensing technology. He received the Global GSP Success Award in 2014.